ACS OMEGA

http://pubs.acs.org/journal/acsodf

Article

Fluorescence Resonance Energy Transfer-Based Aptasensor Made of Carbon-Based Nanomaterials for Detecting Lactoferrin at Low Concentrations

Yingqi Zhang and Jin Zhang*

Cite This: *ACS Omega* 2022, 7, 37964−37970

Read Online

ACCESS | Metrics & More | Article Recommendations | Supporting Information

ABSTRACT: Lactoferrin in the saliva is recently considered a biomarker for the diagnosis of Alzheimer's disease. In this paper, a solution-based, user-friendly biosensing system has been developed to quickly measure lactoferrin at low concentrations. This aptasensor is applied to the fluorescence resonance energy transfer (FRET) quenching mechanism, in which carbon quantum dots (CDs) act as the FRET donor; the FRET quenching element is made of graphene oxide (GO) nanosheets which show good quenching capability. CDs bioconjugated with a chosen aptamer (CDs−aptamer) have the strongest emission (λ_{em}) at 447 nm when excitation (λ_{ex}) is 365 nm. Due to the interaction of the aptamer and GO through the $\pi-\pi^*$ interaction, GO can approach CDs, resulting in FRET quenching. In the presence of lactoferrin, the fluorescence intensity of CDs−aptamer is restored as the binding affinity between lactoferrin and the aptamer is stronger than the $\pi-\pi^*$ interaction between the aptamer and GO. A linear relationship between the restored fluorescence intensity and the concentration of lactoferrin in artificial saliva with a range from 4 to 16 μg/mL is observed. The limit of detection of the solution-based aptasensor is estimated at 2.48 μg/mL. In addition, the sensing performance of the aptasensor made of carbon nanomaterials has been evaluated to test different proteins including major salivary proteins. The results show that this aptasensor has a high selectivity to detect LF with a low concentration, <16 μg/mL.

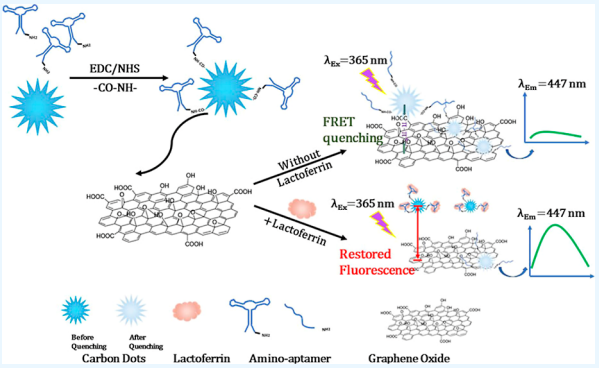

INTRODUCTION

As a member of the transferrin family, lactoferrin (LF) (also known as lactotransferrin) is an iron-binding glycoprotein with a molecular weight of around 80 kDa. It was first isolated from bovine milk in 1939 and from human milk in 1960 by Sorensen and Johanson, respectively.[1] LF shows high anti-inflammatory activity,[2] antioxidant activity,[3] and antimicrobial activity.[4] Previous studies have shown that LF is a suitable biomarker for different diseases, for example, dry eye disease (DED).[5]

Alzheimer's disease (AD) is the most common neuro-degenerative dementia affecting over 50 million people worldwide.[6] The major methods for diagnosis of AD are not easily accessed including magnetic resonance imaging and positron emission tomography (PET), which normally measure the level of cerebrospinal fluid (CSF) tau and amyloid β (Aβ).[7,8] In addition, current methods show relatively low accuracy to the diagnosis of earlier stages of AD.[9] Recently, efforts have been made to study new biomarkers for the early-stage diagnosis of AD. González-Sánchez et al. reported that low salivary LF reflects dysfunctions in the immune system in sporadic Alzheimer's disease.[10] LF is one of the most important defensive elements in saliva because of its excellent antimicrobial activity.[11] Studies indicate that the low level of salivary LF, ∼4.78 μg/mL, often occurs in patients with AD, while it is around 10.24 μg/mL in healthy subjects.[12,13] The significantly reduced level of salivary LF in patients with ADs could be closely related to the brain−immunity interactions, an approach to explain the etiopathogenesis and origin of AD.[13] Compared to CSF total tau and Aβ42 which are measured by current methods for diagnosis of AD, salivary LF could be more accurate as the biomarker for the diagnosis of AD.[12]

Various approaches have been investigated to measure the concentration of LF, including immunoassay (radial immuno-diffusion and enzyme-linked immunosorbent assay) and instrumental analysis [capillary electrophoresis and reversed phase-high-performance liquid chromatography (HPLC)].[18] The major challenge of these reported methods lies in the

Received: August 10, 2022
Accepted: September 22, 2022
Published: October 10, 2022

Scheme 1. Schematic Demonstration of the FRET-Based Aptasensor Made of Carbon Nanomaterials to Detect LF

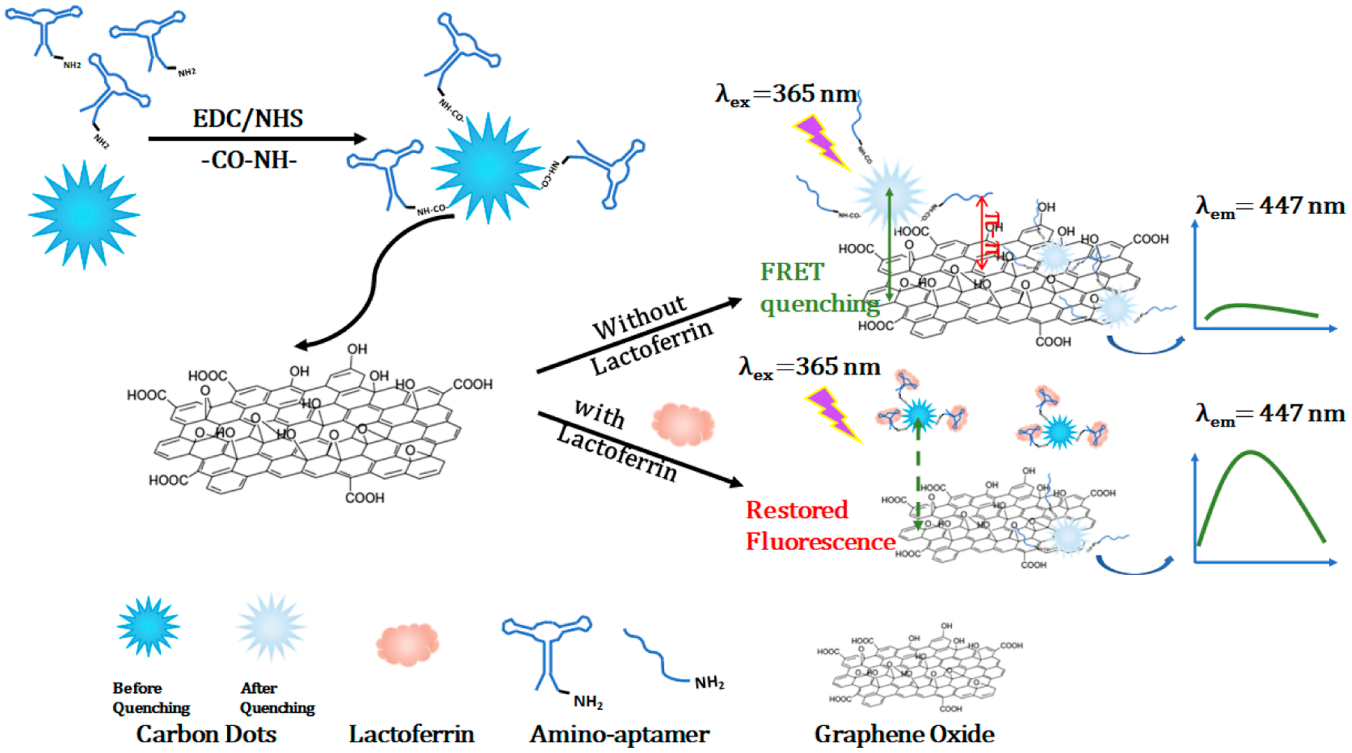

requirement of a bulky and expensive instrument, such as HPLC and GC−MS; furthermore, it takes a long time and requires skills to operate most of the sensing systems available on the market.[14] Consequently, a cost-effective and user-friendly sensing system with quick detection features is needed.

Fluorescence resonance energy transfer (FRET) quenching is a distance-dependent physical energy transfer process in which the energy of the donor can be transferred to the quencher when they are close (<10 nm).[15] The FRET quenching mechanism has been applied in the development of biosensors through integration with nanostructured materials.[16] Carbon-based nanomaterials offer many possibilities in the development of robust sensing systems due to their unique optical, thermal, mechanical, and electrical properties.[17] Carbon quantum dots (CDs) show special properties, for example, tunable photoluminescence (PL), good biocompatibility, and chemical functionalization.[18] Recent study shows that the FRET ratiometric fluorescent probe using CDs as the FRET donor can detect metal ions, that is, Cu^{2+}, in samples from taps and lakes with a limit of detection (LOD) of 0.21 μM.[19] In addition, our previous study on the detection of glucose using CDs with tunable PL as the FRET donor has demonstrated that CDs as the donor in the FRET sensor can quickly measure the tear glucose of streptozotocin-induced diabetic rats in a broad range from 0.2 to 10 mM.[20] On the other hand, graphene oxide (GO), a derivative of graphene, has been considered as an excellent fluorescent quencher because of its wide absorption band from 200 to 800 nm.[21] GO can easily interact with single-stranded DNA (ssDNA) or RNA due to the sp^2 hybridization and $\pi-\pi^*/n-\pi^*$ orbital interactions.[26]

Oligonucleotide aptamers normally have high affinity and selectivity to their corresponding analytes (such as proteins, metal ions, and cells). They can be selected from a library of random oligonucleotide pools using systematic evolution of ligands by exponential enrichment (SELEX). It has been considered a promising alternative to other powerful receptors (such as antibodies) because of the following:[22] (a) high affinity and specificity to identify analytes; (b) high purity and reproducibility for commercial uses; and (c) high flexibility and stability in developing biological applications. In general, a FRET-based aptasensor is constructed by bioconjugating the chosen aptamers onto the FRET donor; a FRET acceptor/quencher coupled with the aptamer will remain at a close distance to the FRET donor.[23]

In this paper, a FRET-based aptasensor has been developed to detect the concentration of LF. As shown in Scheme 1, CDs modified with aptamers (CDs−aptamer) have been produced through the EDC−NHS cross-linking process. GO can reduce the fluorescent intensity of CDs when the oligonucleotide aptamer is absorbed on the surface of GO via $\pi-\pi^*$ interaction. After introducing LF into the biosensing system, the CDs−aptamer is apart from GO because of the strong binding affinity between the aptamer and LF. Therefore, the fluorescence intensity of CDs−aptamer is increased as a function of the concentration of LF. The selectivity of the sensing system has been investigated by measuring different proteins available in saliva. This study could demonstrate a user-friendly and cost-effective biosensing system to measure salivary LF.

EXPERIMENTAL SECTION

Materials and Reagents. Citric acid (251275), urea (U5128), phosphate-buffered saline (PBS) tablet (524650), *N*-(3-dimethylaminopropyl)-*N*′-ethylcarbodiimide hydrochloride (03450), *N*-hydroxysuccinimide (130672), LF from bovine colostrum (L4765), glucose oxidase from *Aspergillus niger* (G7141), concanavalin A-peroxidase from *Canavalia ensiformis* (Jack bean) (L6397), β-casein from bovine milk (C6905),

https://doi.org/10.1021/acsomega.2c05129
ACS Omega 2022, 7, 37964−37970

lysozyme human (L1667), bovine serum albumin (B4287), potassium permanganate (223468), hydrochloric acid (320331), and artificial saliva for pharmaceutical research with pH = 6.8 (SAE0149) were purchased from Sigma-Aldrich. Sulfuric acid was purchased from Caledon Laboratory Chemicals. Graphite flake (43209) was purchased from Alfa Aesar. The LF aptamer with amino modification on the 5′-end was purchased from Integrated DNA Technologies. The sequence used in this study is /5AmMC12/AG GCA GGA CAC CGT AAC CGG TGC ATC TAT GGC TAC TAG CTC TTC CTG CCT.[24]

Synthesis of Carbon Quantum Dots. A microwave-assisted method was used to produce CDs.[25] Citric acid in water (0.5 mL, 0.3 mg/mL) was mixed well with 0.5 mL of 0.3 mg/mL urea in water followed by 5 min of microwave treatment in a 750 W domestic microwave oven. The CDs were obtained after the clear solution changed to a dark-brown clustered solid. The distilled water was used to dissolve this solid and then put into the oven for 2 h at 60 °C to remove residual molecules. Dialysis and centrifugation were applied for purification. The CDs in the powder were obtained using freeze-drying.

Synthesis of Graphene Oxide Nanosheets. GO was prepared based on a modified version of Hummer's method.[26] Graphite flake (1 g) in 50 mL of 98% sulfuric acid solution was put into an ice-water bath for 5 min stirring followed by adding 3 g of potassium permanganate. The solution was kept under 10 °C for 25 min stirring and then treated by ultrasonication for 5 min. The stirring−sonication process required to be repeated 12 times before adding 200 mL of distilled water followed by sonication for 2 h. Finally, GO was washed using 1 M hydrochloric acid solution and distilled water until pH = 6. The powder of GO was obtained using freeze-drying.

Development of the FRET-Based Aptasensor. The optimal ratio of CDs to aptamer was determined by investigation of the absorbance of the aptamer which can be conjugated on CDs (Figure S1). It indicates that 400 μL of the oligonucleotide aptamer with 10 μM concentration was bioconjugated onto 0.4 mg of CDs through EDC−NHS cross-linking, named CDs−aptamer. GO (0.05 mg/mL) suspended in phosphate-buffered saline (PBS) acting as the FRET quenching element was mixed well with CDs−aptamer followed by 20 min incubation at 37 °C to form the solution-based CDs−aptamer−GO sensing system. The optimal ratios of CDs to aptamer and CDs−aptamer to GO have been investigated. LF was diluted using PBS and artificial saliva. Different concentrations of LF in PBS and artificial saliva were added into the sensing system and then incubated at 37 °C for 30 min before measuring the PL under excitation at 365 nm. In addition, the selectivity study was carried out by measuring different proteins under the same conditions. All measures have been tested over three times.

RESULTS AND DISCUSSION

Characterization of CDs and CDs−Aptamer. Figure 1 shows the transmission electron microscopy (TEM) micrograph of CDs, and the small inset image is the high-resolution TEM micrograph of a CD. The average particle size is estimated as 3 ± 1.5 nm. The interplanar *d* spacing is measured at 0.21 nm corresponding to the lattice plane (100) of graphitic carbon.

The LF aptamer molecules have been conjugated onto the CDs through EDC−NHS amidation. The amide bond, −CO−NH−, can be formed through the reaction between the carboxylic groups on the surface of CDs and the amino group modified on the 5′-end of the LF aptamer. FTIR has been employed to study the bioconjugation of the aptamer onto CDs. The typical functional groups on CDs can be identified from Figure 2a. The broad peak centered at 3180 cm^{-1} is

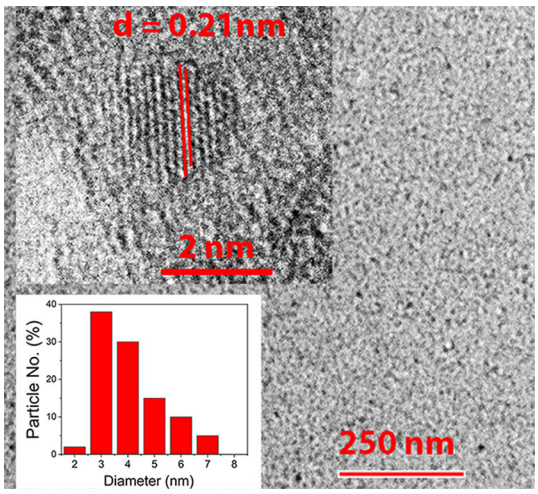

Figure 1. TEM micrograph of CDs; small inset is the HRTEM image of CDs.

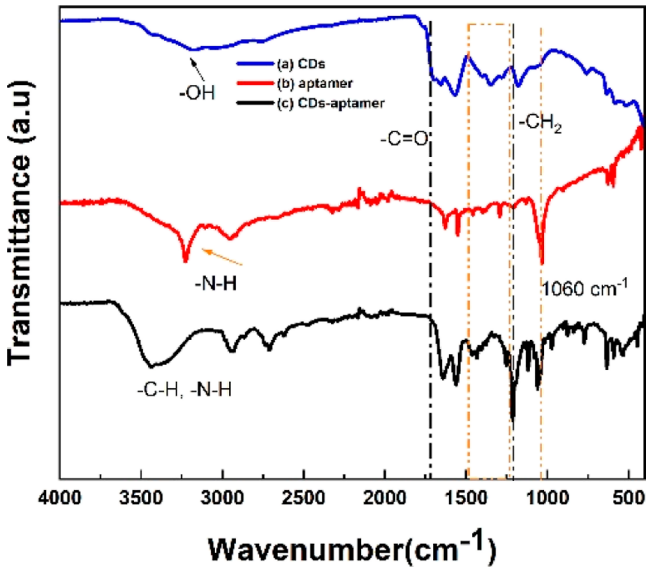

Figure 2. FTIR spectra of (a) CDs, (b) aptamer, and (c) CDs−aptamer.

assigned to the bending vibrations of −OH groups; the band at 1700 cm^{-1} is distributed to the antisymmetric stretches of the carboxylate groups on the surface of CDs.[27] The peaks at 3226 and 1551 cm^{-1} in Figure 2b are attributed to −N−H bending vibration of the amino group modified on the 5′-end aptamer. The wide peak around 3435 cm^{-1} and the strong peak at 1551 cm^{-1} (Figure 2c) are contributed by the amide N−H stretching, and −C−H and C═O stretching, respectively, which demonstrates the successful bioconjugation through forming amide bonds (−CO−NH−).[28] The band located in 1061 cm^{-1} (Figure 2b,c) is attributed to the phosphate band from the nucleic acid backbone.[29] The DNA base−sugar vibration of the aptamer, between 1250 and 1500 cm^{-1}, is

https://doi.org/10.1021/acsomega.2c05129
ACS Omega 2022, 7, 37964−37970

retained when aptamer molecules are bioconjugated onto CDs.[29] It indicates that the structure of the aptamer is retained before and after the bioconjugation to CDs.

Photoluminescence of CDs−Aptamer at Different Excitation Wavelengths. CDs−aptamer has been studied under different excitations (λ_{ex}) from 345 to 465 nm (Figure 3). The emission (λ_{em}) of CDs shifts to right from 437 to 550

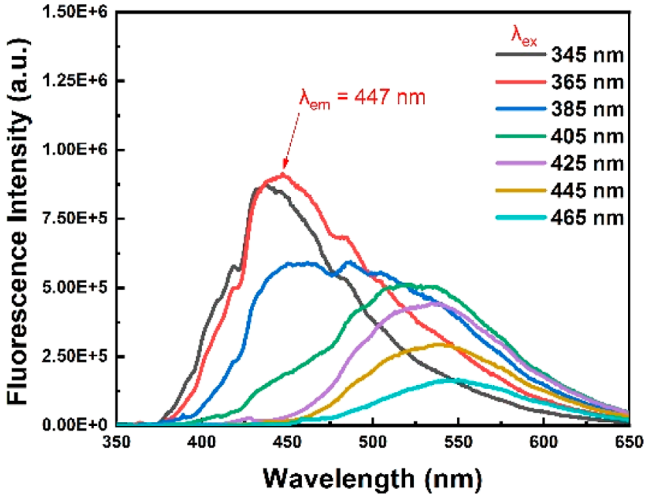

Figure 3. PL of CDs−aptamer under different excitation wavelengths (λ_{ex}) from 345 to 465 nm.

nm, while λ_{ex} increases from 345 to 465 nm; the maximum fluorescence intensity (I_{max}) is observed at λ_{em} = 447 nm when λ_{ex} = 365 nm which is used in the study of the sensor performance for LF detection. The PL of CDs at λ_{ex} = 365 nm has been measured, which shows the same result of PL of CDs−aptamer (Figure S2), and the quantum yield of CDs is calculated as 36% (see the Supporting Information document).

Characterization of GO. Figure 4 shows the UV−vis absorbance spectrum of GO in comparison with the fluorescence emission of CDs when λ_{ex} = 365 nm. The typical absorption peak at 228 nm is attributed to the $\pi-\pi^*$ transitions of the aromatic C−C bond in GO. The shoulder

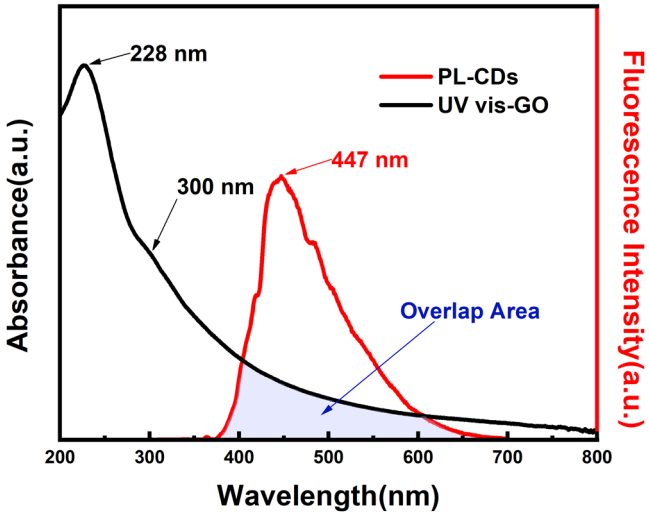

Figure 4. UV−vis absorbance spectrum of GO (blue) and PL of CDs at λ_{ex} = 365 nm (red).

around 300 nm is related to $\pi-\pi^*$ transitions of the C=O bond, which was caused by the oxygen-functional groups on the surface of GO.[30] In addition, a wide range of absorption from 200 to 800 nm is observed which covers the emission of CDs at λ_{em} = 447 nm when λ_{ex} = 365 nm. It indicates that GO has the excellent ability to quench the fluorescence emission of CDs once the distance between them is close, <10 nm through the FRET quenching mechanism.

Optimal Ratio of GO to CDs−Aptamer in the FRET Quenching System. Different concentrations of GO were incubated with the CDs−aptamer to test the ability of GO working as the FRET quenching element. As shown in Figure 5, the I_{max} of CD−aptamer can be decreased by over 47.5%

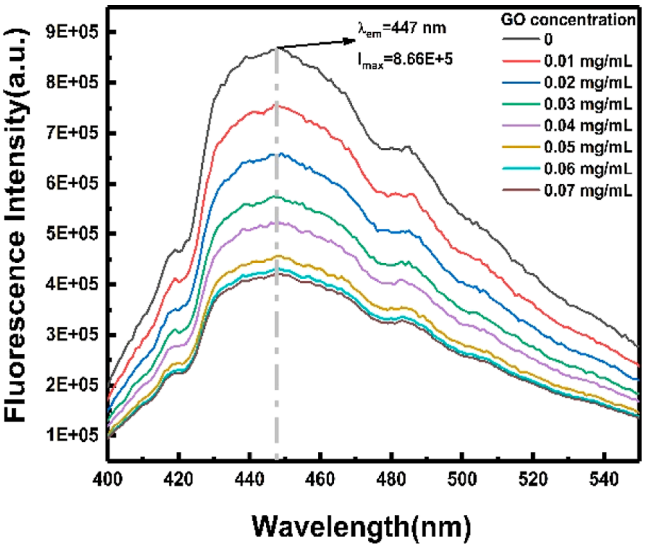

Figure 5. PL of CDs−aptamer under λ_{ex} = 365 nm when the concentration of GO increases.

when the concentration of GO solution increases from 0 to 0.05 mg/mL. A higher concentration (>0.05 mg/mL) of GO could not affect the I_{max} of the CD−aptamer system obviously because of the saturation of the aptamer on CDs interacting with GO through $\pi-\pi^*$ interaction. The result further indicates that FRET quenching occurs in the CDs−aptamer−GO system.

Performance of the FRET Quenching Sensor to Detect LF. Owning to the stronger affinity of the aptamer and LF compared to the interaction between the aptamer and GO, the I_{max} of CDs−aptamer can be restored in the presence of LF.

A good linear relationship between I'_{max}/I_{max} of the CDs−aptamer−GO system and the concentration of LF in the range of 4 to 16 μg/mL is shown in Figure 6a, where I_{max} refers to the I_{max} of the CDs−aptamer−GO system without LF and I'_{max} of the CDs−aptamer−GO system with LF.

In addition, LF diluted within artificial saliva has been investigated to evaluate the sensitivity of the carbon nanostructure-based biosensing system. A similar linear relationship between the restored fluorescence intensity, I'_{max}/I_{max}, of the CDs−aptamer−GO system and the concentration of LF in the range of 4 to 16 μg/mL is shown in Figure 6b. The LOD of the system in detecting LF in artificial saliva is estimated at 2.48 μg/mL. It is also noted that a large error could occur when the concentration of LF is lower which could be improved by adjusting the incubation time. It is

https://doi.org/10.1021/acsomega.2c05129
ACS Omega 2022, 7, 37964−37970

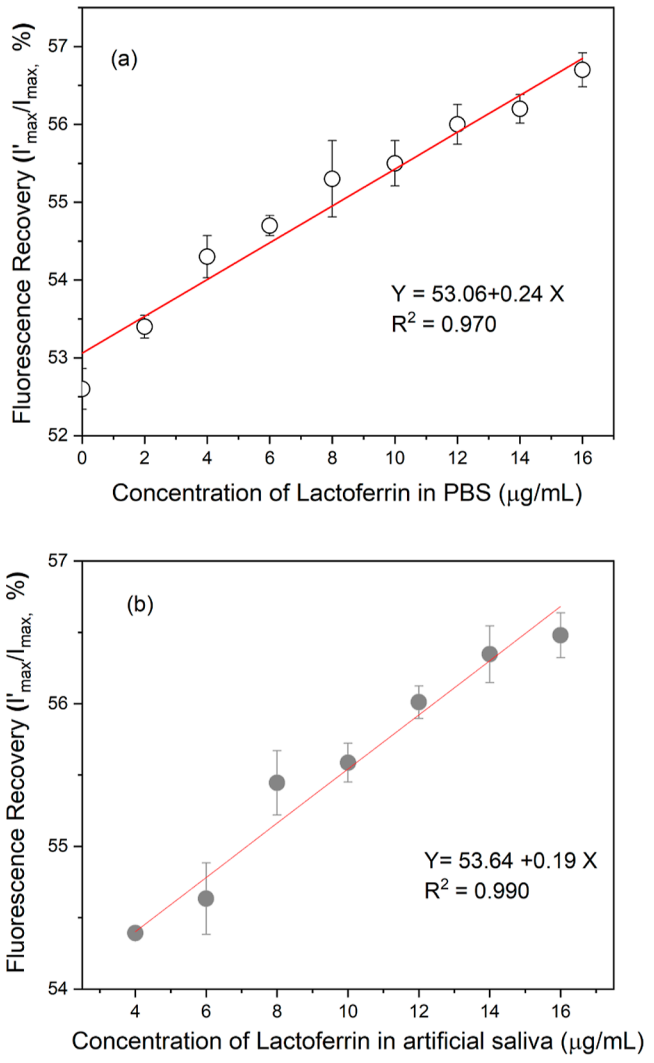

Figure 6. (a) Fluorescence recovery of the biosensing system as a function of the concentration of LF in PBS. (b) Fluorescence recovery of the biosensing system as a function of the concentration of LF in artificial saliva.

noted that artificial saliva has been used as the saliva substitute to treat xerostomia[31] and has been accepted in pharmaceutical research.[32]

Selectivity of the Biosensing System. The selectivity of the CD−aptamer−GO biosensing system has been studied. Figure 7 shows the relative fluorescence recovery of the biosensing system to different proteins including major salivary proteins, LF, lysozyme, peroxidase, β-casein, and albumin in the same concentration, 0.2 μM. In this study, the amount of CDs−aptamer−GO and the volume of the solution remain the same; the relative fluorescence recovery $(F - F_0)/F_0$ is calculated based on the PL of the biosensing system used for detecting different proteins, where F is I_{max} of the biosensing system corresponding to the presence of different proteins and F_0 is the value of I_{max} of the biosensing system without introducing proteins. Compared to other proteins, LF leads to the highest fluorescence recovery of the CDs−aptamer−GO biosensing system.

It is noted that a slightly negative value in the normalized fluorescence recovery occurs when the biosensing system interacts with β-casein. Compared to other proteins, β-casein is

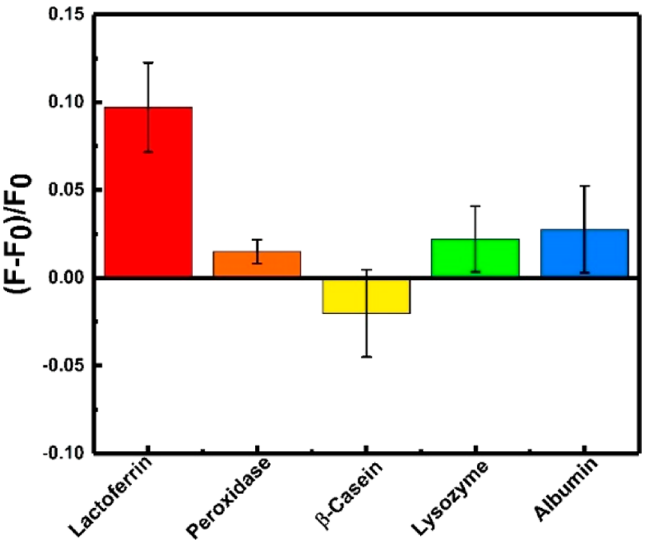

Figure 7. Performance of the designed LF aptasensor responding to different proteins with the same concentration of 0.2 μM. (LF: LF from bovine colostrum; peroxidase: concanavalin A-peroxidase from *Canavalia ensiformis*; β-casein: β-casein from bovine milk; lysozyme: lysozyme human; and albumin: albumin from bovine serum).

a milk protein and has a highly porous structure. Furthermore, it has one tryptophan residue which is sensitive to green light and has a strong UV absorption.[33] The physical interaction between β-casein and the CDs−aptamer−GO system could affect the overall fluorescence properties. On the other hand, the level of salivary proteins can be influenced by the dynamic oral environment. More studies are needed to monitor the level of salivary proteins using such a solution-based biosensing system.

CONCLUSIONS

In summary, a FRET-based aptasensor made of carbon nanomaterials has been developed to detect LF at low concentrations in the aqueous medium. A chosen aptamer that has a strong affinity to LF can be bioconjugated onto CDs through EDC−NHS amidation. The strongest λ_{em} of CDs−aptamer at 447 nm is observed when λ_{ex} = 365 nm. The fluorescence intensity of CDs−aptamer is quenched by GO through FRET quenching because of the short distance between CDs and GO through coupling with the aptamer. It is found that I_{max} of CDs−aptamer has over 47.5% decrease when the concentration of GO in the sensing system increases to 0.05 mg/mL. Due to the competitive reaction between LF and GO to react with the aptamer, the aptasensor, CDs−aptamer−GO, can be used to detect LF by applying the FRET quenching mechanism. In the presence of LF, the fluorescence intensity is restored due to the stronger binding affinity between LF and the aptamer. A linear relationship between the fluorescence recovery and the concentration of LF in artificial saliva within the range of 4 to 16 μg/mL is observed. The LOD of the FRET-based aptasensor is estimated at 2.48 μg/mL for detecting LF in artificial saliva. The sensing range covers the concentration of salivary LF in the healthy subject, 10.24 μg/mL, and patients with AD, 4.78 μg/mL. The aptasensor made of carbon nanomaterials shows high selectivity to LF detection.

https://doi.org/10.1021/acsomega.2c05129
ACS Omega 2022, 7, 37964−37970

■ ASSOCIATED CONTENT

Supporting Information

The Supporting Information is available free of charge at https://pubs.acs.org/doi/10.1021/acsomega.2c05129.

Optimal ratio of the aptamer to CDs, photoluminescence of CDs, and quantum yield of CDs (PDF)

■ AUTHOR INFORMATION

Corresponding Author

Jin Zhang − *Department of Chemical and Biochemical Engineering, University of Western Ontario, London, Ontario N6A 5B9, Canada;* orcid.org/0000-0002-6875-8008; Email: jzhang@eng.uwo.ca

Author

Yingqi Zhang − *Department of Chemical and Biochemical Engineering, University of Western Ontario, London, Ontario N6A 5B9, Canada*

Complete contact information is available at: https://pubs.acs.org/10.1021/acsomega.2c05129

Author Contributions

Y.Z.: conceptualization, methodology, software, investigation, validation, formal analysis, and writing: original draft. J.Z.: conceptualization, methodology, funding acquisition supervision, and writing: review and editing.

Notes

The authors declare no competing financial interest.

■ ACKNOWLEDGMENTS

This study was funded by the Natural Sciences and Engineering Research Council of Canada (NSERC).

■ REFERENCES

(1) Sorensen, M.; Sorensen, S. The proteins in whey. *Compte rendu des Travaux du Laboratoire de Carlsberg, Ser. Chim.* **1940**, *23*, 55−99. Johanson, B. Isolation of an iron-containing red protein from milk. *Acta Chem. Scand.* **1960**, *14*, 510−512.

(2) Conneely, O. M. Antiinflammatory activities of lactoferrin. *J. Am. Coll. Nutr.* **2001**, *20*, 389S−395S.

(3) Safaeian, L.; Zabolian, H. Antioxidant effects of bovine lactoferrin on dexamethasone-induced hypertension in rat. *Int. Scholarly Res. Not.* **2014**, *2014*, 943523.

(4) Jenssen, H.; Hancock, R. E. Antimicrobial properties of lactoferrin. *Biochimie* **2009**, *91*, 19−29.

(5) Boukes, R.; Boonstra, A.; Breebaart, A.; Reits, D.; Glasius, E.; Luyendyk, L.; Kijlstra, A. Analysis of human tear protein profiles using high performance liquid chromatography (HPLC). *Doc. Ophthalmol.* **1987**, *67*, 105−113.

(6) Kincaid, H. J.; Nagpal, R.; Yadav, H. Diet-microbiota-brain axis in Alzheimer's disease. *Ann. Nutr. Metab.* **2021**, *77*, 21−27.

(7) Chandra, A.; Dervenoulas, G.; Politis, M. Magnetic resonance imaging in Alzheimer's disease and mild cognitive impairment. *J. Neurol.* **2019**, *266*, 1293−1302.

(8) Chen, D.-W.; Wang, J.; Zhang, L.-L.; Wang, Y.-J.; Gao, C.-Y. Cerebrospinal fluid amyloid-β levels are increased in patients with insomnia. *J. Alzheimer's Dis.* **2018**, *61*, 645−651. Hulstaert, F.; Blennow, K.; Ivanoiu, A.; Schoonderwaldt, H.; Riemenschneider, M.; Deyn, P.; Bancher, C.; Cras, P.; Wiltfang, J.; Mehta, P.; Iqbal, K.; Pottel, H.; Vanmechelen, E.; Vanderstichele, H. Improved discrimination of AD patients using β-amyloid (1-42) and tau levels in CSF. *Neurology* **1999**, *52*, 1555.

(9) Galvin, J. E.; Aisen, P.; Langbaum, J. B.; Rodriguez, E.; Sabbagh, M.; Stefanacci, R.; Stern, R. A.; Vassey, E. A.; de Wilde, A.; West, N. Early stages of alzheimer's disease: Evolving the care team for optimal patient management. *Front. Neurol.* **2021**, *11*, 592302. Leszek, J.; Md Ashraf, G.; Tse, W. H.; Zhang, J.; Gasiorowski, K.; Avila-Rodriguez, M. F.; Tarasov, V. V.; Barreto, G. E.; Klochkov, S. G.; Bachurin, S. O.; Aliev, G. Nanotechnology for Alzheimer disease. *Curr. Alzheimer Res.* **2017**, *14*, 1182−1189.

(10) González-Sánchez, M.; Bartolome, F.; Antequera, D.; Puertas-Martín, V.; González, P.; Gómez-Grande, A.; Llamas-Velasco, S.; Herrero-San Martín, A.; Pérez-Martínez, D.; Villarejo-Galende, A. Decreased salivary lactoferrin levels are specific to Alzheimer's disease. *EBioMedicine* **2020**, *57*, 102834.

(11) Welling, M. M.; Nabuurs, R. J.; Weerd, L. Potential role of antimicrobial peptides in the early onset of Alzheimer's disease. *Alzheimer's Dementia* **2015**, *11*, 51−57.

(12) Carro, E.; Bartolomé, F.; Bermejo-Pareja, F.; Villarejo-Galende, A.; Molina, J. A.; Ortiz, P.; Calero, M.; Rabano, A.; Cantero, J. L.; Orive, G. Early diagnosis of mild cognitive impairment and Alzheimer's disease based on salivary lactoferrin. *Alzheimer's Dement.: Diagn. Assess.* **2017**, *8*, 131−138.

(13) Antequera, D.; Moneo, D.; Carrero, L.; Bartolome, F.; Ferrer, I.; Proctor, G.; Carro, E. Salivary Lactoferrin Expression in a Mouse Model of Alzheimer's Disease. *Front. Immunol.* **2021**, *12*, 4054. Bermejo Pareja, F.; Del Ser, T.; Valentí, M.; de la Fuente, M.; Bartolome, F.; Carro, E. Salivary lactoferrin as biomarker for Alzheimer's disease: Brain-immunity interactions. *Alzheimer's Dementia* **2020**, *16*, 1196−1204.

(14) Zhang, Y.; Lu, C.; Zhang, J. Lactoferrin and Its Detection Methods: A Review. *Nutrients* **2021**, *13*, 2492.

(15) Johansson, M. K.; Fidder, H.; Dick, D.; Cook, R. M. Intramolecular dimers: a new strategy to fluorescence quenching in dual-labeled oligonucleotide probes. *J. Am. Chem. Soc.* **2002**, *124*, 6950−6956.

(16) Chen, L.; Tse, W. H.; Chen, Y.; McDonald, M. W.; Melling, J.; Zhang, J. Nanostructured biosensor for detecting glucose in tear by applying fluorescence resonance energy transfer quenching mechanism. *Biosens. Bioelectron.* **2017**, *91*, 393−399.

(17) Maiti, D.; Tong, X.; Mou, X.; Yang, K. Carbon-based nanomaterials for biomedical applications: a recent study. *Front. Pharmacol.* **2019**, *9*, 1401−1416.

(18) Ji, C.; Zhou, Y.; Leblanc, R. M.; Peng, Z. Recent developments of carbon dots in biosensing: A review. *ACS Sens.* **2020**, *5*, 2724−2741.

(19) Yan, F.; Bai, Z.; Chen, Y.; Zu, F.; Li, X.; Xu, J.; Chen, L. Ratiometric fluorescent detection of copper ions using coumarin-functionalized carbon dots based on FRET. *Sens. Actuators, B* **2018**, *275*, 86−94.

(20) Chen, L.; Dotzert, M.; Melling, C. J.; Zhang, J. Tunable Photoluminescence of Carbon Dots used for Homogeneous Glucose Sensing Assay. *Biochem. Eng. J.* **2020**, *159*, 107580.

(21) Liu, B.; Salgado, S.; Maheshwari, V.; Liu, J. DNA adsorbed on graphene and graphene oxide: Fundamental interactions, desorption and applications. *Curr. Opin. Colloid Interface Sci.* **2016**, *26*, 41−49.

(22) Song, S.; Wang, L.; Li, J.; Fan, C.; Zhao, J. Aptamer-based biosensors. *TrAC, Trends Anal. Chem.* **2008**, *27*, 108−117.

(23) Pehlivan, Z. S.; Torabfam, M.; Kurt, H.; Ow-Yang, C.; Hildebrandt, N.; Yüce, M. Aptamer and nanomaterial based FRET biosensors: a review on recent advances (2014−2019). *Microchim. Acta* **2019**, *186*, 563.

(24) Liu, X.; Li, H.; Jia, W.; Chen, Z.; Xu, D. Selection of aptamers based on a protein microarray integrated with a microfluidic chip. *Lab Chip* **2017**, *17*, 178−185. Chen, Z.; Li, H.; Jia, W.; Liu, X.; Li, Z.; Wen, F.; Zheng, N.; Jiang, J.; Xu, D. Bivalent aptasensor based on silver-enhanced fluorescence polarization for rapid detection of lactoferrin in milk. *Anal. Chem.* **2017**, *89*, 5900−5908.

(25) Qu, S.; Wang, X.; Lu, Q.; Liu, X.; Wang, L. A biocompatible fluorescent ink based on water-soluble luminescent carbon nanodots. *Angew. Chem., Int. Ed.* **2012**, *51*, 12215−12218.

(26) Abdolhosseinzadeh, S.; Asgharzadeh, H.; Seop Kim, H. Fast and fully-scalable synthesis of reduced graphene oxide. *Sci. Rep.* **2015**, *5*, 10160.
(27) Ţucureanu, V.; Matei, A.; Avram, A. M. FTIR spectroscopy for carbon family study. *Crit. Rev. Anal. Chem.* **2016**, *46*, 502−520.
(28) Haris, P. I.; Chapman, D. The conformational analysis of peptides using Fourier transform IR spectroscopy. *Biopolymers* **1995**, *37*, 251−263.
(29) Dovbeshko, G. I.; Gridina, N. Y.; Kruglova, E. B.; Pashchuk, O. P. FTIR spectroscopy studies of nucleic acid damage. *Talanta* **2000**, *53*, 233−246.
(30) Chaiyakun, S.; Witit-Anun, N.; Nuntawong, N.; Chindaudom, P.; Oaew, S.; Kedkeaw, C.; Limsuwan, P. Preparation and characterization of graphene oxide nanosheets. *Procedia Eng.* **2012**, *32*, 759−764.
(31) Davies, A.; Singer, J. A comparison of artificial saliva and pilocarpine in radiation induced xerostomia. *J. Laryngol. Otol.* **1994**, *108*, 663−665.
(32) Pistone, S.; Goycoolea, F. M.; Young, A.; Smistad, G.; Hiorth, M. Formulation of polysaccharide-based nanoparticles for local administration into the oral cavity. *Eur. J. Pharm. Sci.* **2017**, *96*, 381−389.
(33) Bourassa, P.; Bekale, L.; Tajmir-Riahi, H. A. Association of lipids with milk α- and β-caseins. *Int. J. Biol. Macromol.* **2014**, *70*, 156−166.

https://doi.org/10.1021/acsomega.2c05129
ACS Omega 2022, 7, 37964−37970